Unique COPII component AtSar1a/AtSec23a pair is required for the distinct function of protein ER export in *Arabidopsis thaliana*

Yonglun Zeng[a], Kin Pan Chung[a], Baiying Li[a], Ching Man Lai[a,b], Sheung Kwan Lam[c], Xiangfeng Wang[a], Yong Cui[a], Caiji Gao[a], Ming Luo[a], Kam-Bo Wong[b], Randy Schekman[c], and Liwen Jiang[a,d,1]

[a]School of Life Sciences, Centre for Cell and Developmental Biology and State Key Laboratory of Agrobiotechnology, The Chinese University of Hong Kong, Shatin, New Territories, Hong Kong SAR, China; [b]School of Life Sciences, Center for Protein Science and Crystallography, The Chinese University of Hong Kong, Shatin, New Territories, Hong Kong SAR, China; [c]Department of Molecular and Cell Biology, Howard Hughes Medical Institute, University of California, Berkeley, CA 94720; and [d]Shenzhen Research Institute, The Chinese University of Hong Kong, Shenzhen 518057, China

Edited by Natasha V. Raikhel, Center for Plant Cell Biology, Riverside, CA, and approved October 9, 2015 (received for review October 3, 2015)

Secretory proteins traffic from endoplasmic reticulum (ER) to Golgi via the coat protein complex II (COPII) vesicle, which consists of five cytosolic components (Sar1, Sec23-24, and Sec13-31). In eukaryotes, COPII transport has diversified due to gene duplication, creating multiple COPII paralogs. Evidence has accumulated, revealing the functional heterogeneity of COPII paralogs in protein ER export. Sar1B, the small GTPase of COPII machinery, seems to be specialized for large cargo secretion in mammals. *Arabidopsis* contains five Sar1 and seven Sec23 homologs, and AtSar1a was previously shown to exhibit different effects on α-amylase secretion. However, mechanisms underlying the functional diversity of Sar1 paralogs remain unclear in higher organisms. Here, we show that the *Arabidopsis* Sar1 homolog AtSar1a exhibits distinct localization in plant cells. Transgenic *Arabidopsis* plants expressing dominant-negative AtSar1a exhibit distinct effects on ER cargo export. Mutagenesis analysis identified a single amino acid, Cys84, as being responsible for the functional diversity of AtSar1a. Structure homology modeling and interaction studies revealed that Cys84 is crucial for the specific interaction of AtSar1a with AtSec23a, a distinct *Arabidopsis* Sec23 homolog. Structure modeling and coimmunoprecipitation further identified a corresponding amino acid, Cys484, on AtSec23a as being essential for the specific pair formation. At the cellular level, the Cys484 mutation affects the distinct function of AtSec23a on vacuolar cargo trafficking. Additionally, dominant-negative AtSar1a affects the ER export of the transcription factor bZIP28 under ER stress. We have demonstrated a unique plant pair of COPII machinery function in ER export and the mechanism underlying the functional diversity of COPII paralogs in eukaryotes.

coat protein complex II | Sar1 | Sec23 | ER export | functional diversity

The molecular basis for protein export out of the endoplasmic reticulum (ER) has been built on the isolation and characterization of *sec* mutants that accumulate ER membranes at the nonpermissive temperature in yeast (1). The vesicle coat proteins responsible for ER-Golgi transport, collectively termed the "coat protein complex II" (COPII), were discovered by combining this genetic approach with biochemical assays (2). The COPII vesiculating machinery consists of five cytosolic proteins: Sar1, Sec23, Sec24, Sec13, and Sec31. The small GTPase Sar1 (Secretion-associated and RAS superfamily-related protein 1) (3) is first activated and recruited to the ER membrane by the guanosine nucleotide exchange factor Sec12, an ER-localized integral membrane protein (4). Subsequently, the GTPase activating protein (GAP) Sec23, which stimulates the enzymatic activity of Sar1 (5), and the adaptor protein Sec24 (6), are recruited to the ER membrane as a heterodimer by Sar1-GTP to form a prebudding complex (7). This complex in turn recruits a Sec13/Sec31 heterotetramer, which forms the outer layer of the COPII coat, completing the vesicle formation process.

In mammals, COPII transport has diversified due to gene-duplication events, creating multiple paralogs of four of the COPII proteins, except for Sec13. Elucidating the reason for the existence and conservation of multiple paralogs in higher organisms poses a major challenge. Recently, mutations of some COPII paralogs including Sec23A, Sec23B, and Sec24B have been shown to cause distinct developmental disorders and human diseases (8). More interestingly, even though sharing high sequence identity with Sar1A, human Sar1B seems to be specialized to enable the ER export of large cargo chylomicrons (9). Different mutations in Sar1B are associated with lipid absorption disorders due to defects in chylomicron secretion: Anderson disease and chylomicron retention disease (9). However, mechanism underlying the distinct functions of human Sar1 homologs remains unclear.

In *Arabidopsis*, COPII isoforms are greater in number than in other eukaryotes. There are five Sar1, two Sec13, two Sec31, seven Sec23, and three Sec24 isoforms (10). However, the significance of this diversification remains unresolved, raising the question as to whether tissue specificity or functional diversity exists for plant COPII isoforms. So far, only two studies have pointed toward a functional diversity for COPII homologs in *Arabidopsis*. Genetic screening has identified a recessive mis-sense point mutation (R693K) in Sec24A, which induces the formation of ER and Golgi membrane clusters and leads to a partial redistribution of Golgi and secretory markers in the clusters (11, 12). Interestingly, the expression of Sec24A or YFP-Sec24A complemented the mis-sense mutation phenotype but did not occur with Sec24B and Sec24C, indicating the existence of functional diversity among the *Arabidopsis* Sec24 paralogs. More strikingly, transient expression experiments in tobacco protoplasts have shown that AtSar1a (At1g09180), which shares a 93% amino acid sequence identity

Significance

The underlying mechanisms causing the functional diversity of small GTPase Sar1 paralogs in coat protein complex II-mediated protein endoplasmic reticulum (ER) export remain elusive in higher organisms. *Arabidopsis* contains five Sar1 homologs. In this study, we show that AtSar1a exhibits a distinct localization and effects on ER cargo export in plants through a unique interaction with the COPII coat protein AtSec23a. This specific pairing is required for the distinct function in ER export under ER stress in *Arabidopsis*. Our results point to a mechanism underlying the functional diversity of COPII paralogs in eukaryotes.

Author contributions: Y.Z., K.-B.W., R.S., and L.J. designed research; Y.Z., K.P.C., B.L., C.M.L., S.K.L., X.W., Y.C., C.G., and M.L. performed research; Y.Z., C.M.L., and K.-B.W. analyzed data; and Y.Z. and L.J. wrote the paper.

The authors declare no conflict of interest.

This article is a PNAS Direct Submission.

[1]To whom correspondence should be addressed. Email: ljiang@cuhk.edu.hk.

This article contains supporting information online at www.pnas.org/lookup/suppl/doi:10.1073/pnas.1519333112/-/DCSupplemental.

with other *Arabidopsis* Sar1 homologs, exhibited different effects on the secretion of a soluble secretory reporter α-amylase (13). However, the mechanisms underlying the functional diversity of the AtSar1a in the proteins ER export remain to be elucidated.

Here, we report that the AtSar1a (At1g09180) exhibits a distinct ER exit site localization that is closely associated with the Golgi apparatus in plant cells. We further demonstrate that a dominant-negative mutant of AtSar1a showed distinct effects on the ER export of vacuolar and membrane cargos in *Arabidopsis*, which is determined by a single amino acid substitution from the conserved tyrosine to cysteine at position 84 on AtSar1a. Homology modeling and interaction assays have proved that the amino acid Cys84 is crucial for the specific interaction of AtSar1a with AtSec23a (accession no. At4g01810), a distinct *Arabidopsis* Sec23 homolog. Strikingly, protein structure modeling showed that only AtSec23a contains a corresponding amino acid substitution from conserved aspartate to cysteine at position 484, which contacts with Cys84 on AtSar1a. This specific amino acid Cyc484 on AtSec23a was further shown to be essential for the specific interaction with AtSar1a and contributes to the unique function of AtSec23a on ER vacuolar cargo export together with AtSar1a. Under ER stress, dominant-negative AtSar1a affects the ER export of a transcription factor bZIP28, an ER resident stress sensor/transducer related to mammalian ATF6. Thus, our data reveal a plant unique pair of COPII machinery function in ER export and the mechanism underlying the functional diversity of COPII paralogs in eukaryotes.

Results and Discussion

AtSar1a Has a Distinct ER Exit Site Localization in Plants. In eukaryotes, the export of proteins from the ER is facilitated by COPII vesicles, which are formed at ER exit sites (ERES) (14). In mammals, ERES are frequently associated with the ER-Golgi intermediate compartment (ERGIC). The presence of ERGIC in higher plant cells remains elusive but a recent study suggests that the SYP31 compartment may represent a scaffold to build the Golgi stack, similar to the ERGIC in mammals (15). COPII components have been used as markers to study ERES in plants with various working models on the spatial relationship between ERES and Golgi (16). An advanced "hybrid model" was recently proposed, suggesting that ERES may have two different populations: those continuously associated with Golgi or those without associated Golgi stacks (17).

The *Arabidopsis* genome encodes five putative Sar1 proteins (10). Among them, AtSar1a and AtSar1b were shown to exhibit ERES localization and Golgi association in tobacco leaf epidermal cells when transiently coexpressing with Golgi proteins (13). Immunofluorescence labeling with AtSar1b antibodies suggested that the AtSar1b-labeled puncta are more abundant than the Golgi apparatus in tobacco BY-2 cells and leaf pavement cells (18, 19). To investigate the possibility that *Arabidopsis* Sar1 homologs have different localizations, we generated transgenic *Arabidopsis* plants expressing green fluorescent protein (GFP)-tagged AtSar1a and AtSar1c (accession no. At4g02080) driven by a ubiquitin promoter and performed an immunofluorescence labeling analysis. Consistent with previous studies (18, 20, 21), we found that overexpression of AtSar1a-GFP and AtSar1c-GFP did not affect plant growth and their protein distribution (*SI Appendix*, Fig. S1 *A* and *B*). To confirm that the punctate structures labeled by AtSar1a-GFP and AtSar1c-GFP are bona fide COPII assembly sites, we treated the transgenic plants with H89, the protein kinase inhibitor used to inhibit Sar1 and COPII assembly onto the ER membrane (22). The punctae labeled by AtSar1a-GFP and AtSar1c-GFP gradually decreased upon treatments with increasing concentrations of H89 (*SI Appendix*, Fig. S2*A*). Immunoblot analysis showed that the membrane-bound AtSar1a-GFP and AtSar1c-GFP decreased with H89 treatments compared with the untreated controls (*SI Appendix*, Fig. S2 *B* and *C*). To examine their subcellular localization, we performed immunofluorescence labeling with an antibody against the endogenous *cis*-Golgi protein EMP12 and showed that AtSar1c localized at puncta only partially overlapped with EMP12 and was mainly separate from the Golgi apparatus in *Arabidopsis* root cells (Fig. 1 *Aa* and *B*). Similar results were also obtained with AtSar1c-GFP transgenic tobacco BY-2 cell lines (Fig. 1 *Ca* and *D*). These results are consistent with previous studies that showed that AtSar1b only partially overlapped with the Golgi apparatus in plant cells (18, 19). Interestingly, AtSar1a exhibited a distinct localization in both *Arabidopsis* root cells (Fig. 1 *Ab* and *B*) and tobacco BY-2 cells (Fig. 1 *Cb* and *D*), as most puncta labeled by AtSar1a were peri-Golgi localized. To further confirm the results, we performed superresolution microscopy [structured illumination microscopy (SIM)] with AtSar1a-GFP– and AtSar1c-GFP–transfected *Arabidopsis* protoplasts. AtSar1a-labeled puncta were closely associated with the Golgi marker whereas the AtSar1c-GFP positive punctae were largely separated from the Golgi apparatus (Fig. 1*E*). The observation on the association of AtSar1a punctate with the Golgi apparatus is consistent with previous studies using superresolution microscopy that showed that ERES are surrounded by the Golgi apparatus and that ERES shows more numbers than the Golgi (15, 23). In contrast, most of the AtSar1c-GFP–labeled punctae were not Golgi-associated under superresolution microscopy. Thus, our results showed that AtSar1a has a distinct localization in plant cells, which may specifically represent active peri-Golgi ERES. This seems to be consistent with the high expression profile of AtSar1a in pollen (10), whose rapid and polarized growth demand an active secretory system. Furthermore, distinct

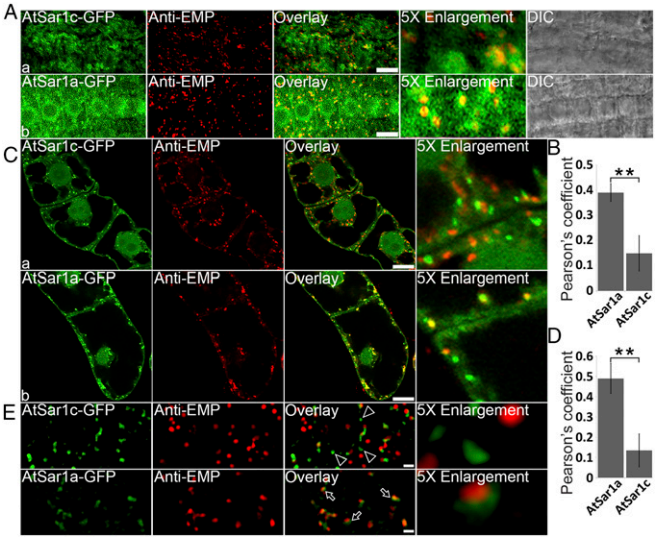

Fig. 1. AtSar1a localizes at distinct population of ERESs in *Arabidopsis* plants and transgenic tobacco BY-2 cells. (*A*) Confocal immunofluorescence labeling of AtSar1c-GFP and AtSar1a-GFP transgenic *Arabidopsis* plants in root cells with the *cis*-Golgi marker anti-EMP. (*a*) AtSar1c-GFP–labeled punctae revealed a less peri-Golgi pattern whereas (*b*) AtSar1a-GFP–labeled punctate structures were found mainly in the peri-Golgi area. (Scale bars, 10 μm.) (*B*) Pearson colocalization coefficients of AtSar1c and AtSar1a with the *cis*-Golgi protein EMP as shown in *A* were quantified ($n = 3$ independent experiments; $n \geq 3$ cells were assessed per independent experiment). Data represent mean ± SD $^{**}P < 0.01$ (two-tailed *t* test). (*C*) Confocal immunofluorescence labeling of AtSar1c-GFP and AtSar1a-GFP transgenic tobacco BY-2 cells with the *cis*-Golgi EMP-antibody. (Scale bars, 10 μm.) (*D*) Pearson colocalization coefficients of AtSar1c and AtSar1a with the *cis*-Golgi protein EMP as shown in *C* were quantified as in *B*. (*E*) Superresolution (*N*-SIM) observation of the spatial relationship between AtSar1c-GFP or AtSar1a-GFP and Golgi in *Arabidopsis* protoplasts. Arrowheads indicate examples of AtSar1c-GFP–positive punctae without Golgi association. Arrows indicate examples of Golgi-associated punctate structures labeled by AtSar1a-GFP. (Scale bars, 1 μm.)

PLANT BIOLOGY

ERES specialized for the export of different ER cargos have been visualized in budding yeast (24). The recent "hybrid model" for the ERES and Golgi organization in plant cells also indicates that there may be different ERES populations (17). Thus, our findings may indicate the existence of different types of ERES in higher plants and the dedication of AtSar1a to distinct cargoes of ER export.

A Single Amino Acid Determines the Distinct Effects of AtSar1a on Protein ER Export. A previous study has shown that expression of the dominant mutant of *Arabidopsis* Sar1 GTPase (AtSar1 H74L) inhibits ER-Golgi transport in plant cells (25). To examine the possibility that AtSar1a might perform a different function in protein ER export in *Arabidopsis*, we generated transgenic *Arabidopsis* plants expressing a AtSar1a dominant-negative mutant (AtSar1aDN)-GFP and a AtSar1c dominant-negative mutant (AtSar1cDN)-GFP, each under the control of a dexamethasone (DEX)-inducible promoter. When triggered with DEX, ER export of the vacuolar cargo Aleurain-mRFP introduced into seedlings by particle bombardment was inhibited in the dex::AtSar1cDN-GFP transgenic plants (*SI Appendix*, Fig. 2*Aa*), whereas the Aleurain-mRFP still reached the vacuole in the dex::AtSar1aDN-GFP mutants (*SI Appendix*, Fig. 2*Ab*). Meanwhile, ER export of the Aleurain-mRFP was not affected either in AtSar1a-GFP and AtSar1c-GFP transgenic plants or in protoplasts coexpressing the AtSar1a-GFP and AtSar1c-GFP fusions (*SI Appendix*, Fig. S1*C*). Similar results were obtained from the transient expression assay using *Arabidopsis* plant system biology dark-type culture protoplasts (*SI Appendix*, Fig. S3 *A*, *B*, *C*, and *F*). Consistently, immunoblot analysis showed that overexpression of AtSar1cDN-GFP caused the full-length Aleurain-mRFP to be retained in the transfected *Arabidopsis* protoplasts, whereas Aleurain-mRFP was degraded to the RFP core in the vacuole when coexpressed with AtSar1aDN-GFP (*SI Appendix*, Fig. S3*G*). These results indicated that AtSar1aDN exhibited distinct effects on ER cargo export in both *Arabidopsis* protoplasts and plants compared with other *Arabidopsis* Sar1 paralogs, which is consistent with a previous study in tobacco leaf protoplasts (13).

To elucidate the mechanism underlying the distinct effects of AtSar1a on ER protein export, we performed gene-swapping analysis as previously described (26) to find out which domain or amino acids cause the functional heterogeneity of AtSar1a. *Arabidopsis* plants expressing a chimera of 1–90 amino acids from AtSar1aDN and 91–193 amino acids from AtSar1c driven by the DEX inducible promoter, were generated [dex::AtSar1aDN N terminus (NT)-GFP transgenic plants]. Interestingly, Aleurain-mRFP was correctly transported to the vacuole in the dex::AtSar1aDN NT-GFP mutant plants upon DEX induction (Fig. 2*Ac*). Similarly, when transiently coexpressed with AtSar1aDN NT-GFP in *Arabidopsis* protoplasts, Aleurain-mRFP was normally delivered to the vacuole (*SI Appendix*, Fig. S3 *E* and *F*). In contrast, the vacuolar cargo was trapped in the ER when coexpressed with AtSar1cDN NT-GFP, which is the chimera of 1–90 amino acids from AtSar1cDN and 91–193 amino acids from AtSar1a (*SI Appendix*, Fig. S3 *D* and *F*). These results were further supported by immunoblot analysis in *Arabidopsis* protoplasts (*SI Appendix*, Fig. S3*G*). Thus, the N terminus contains the key element for AtSar1a function. To further identify which amino acids in the N terminus are crucial for the distinct effects of AtSar1a on ER protein export, we next performed point mutagenesis on the AtSar1aDN according to the protein sequence of other *Arabidopsis* Sar1 homologs (*SI Appendix*, Fig. S4*A*). Strikingly, when coexpressed with AtSar1aDN C84Y-GFP, in which the cysteine at position 84 of AtSar1aDN was mutated to the conserved tyrosine of other Sar1 homologs at that position (*SI Appendix*, Fig. S4*B*), the vacuolar cargo Aleurain-mRFP was trapped in the ER in *Arabidopsis* protoplasts (*SI Appendix*, Fig. S4*C*). To our surprise, Aleurain-mRFP was still normally delivered to the vacuole when coexpressed with other point mutation constructs of

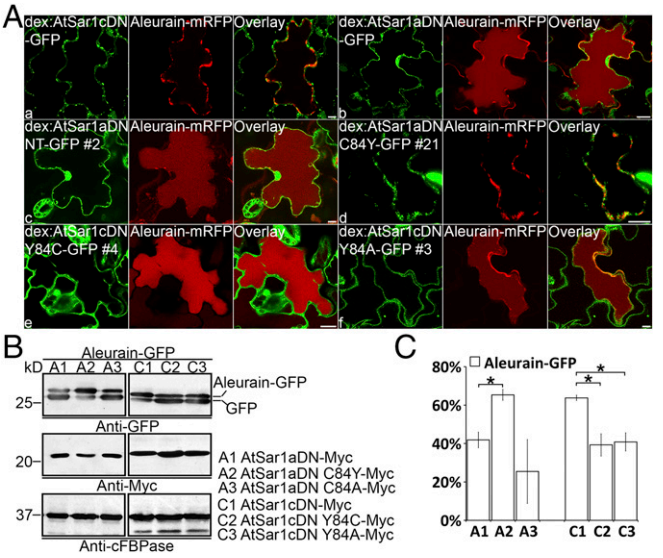

Fig. 2. A single amino acid substitution determines the distinct effects of AtSar1a on ER vacuolar cargo export. (*A*) Subcellular localization of the vacuolar cargo proteins Aleurain-mRFP in transgenic plants expressing DEX-inducible GFP fusions of various AtSar1s. (Scale bars, 10 μm.) (*B*) Transient-trafficking assays of vacuolar cargo proteins. Aleurain-GFP was cotransformed with Myc-tag mutants of AtSar1a (A1–A3) or AtSar1c (C1–C3) in *Arabidopsis* protoplasts, which were subjected to protein extraction and immunoblot analysis using indicated antibodies. The data shown are from a single representative experiment of three repeats. (*C*) The relative grayscale intensity (scale 0–100%) of Aleurain-GFP was quantified using ImageJ software in which the combinatorial intensity of both Aleurain-GFP and the GFP core was expressed as 100% ($n = 3$ independent experiments). Data represent mean ± SD; $^*P < 0.05$ (ANOVA with Scheffé test).

AtSar1aDN (*SI Appendix*, Fig. S5*A*). Consistently, immunoblot analysis showed that Aleurain-mRFP was degraded to the RFP core in the vacuole when coexpressed with other AtSar1aDN-GFP point mutations in protoplasts (*SI Appendix*, Fig. S5*B*). To further confirm that a single amino acid at position 84 determines the distinct function of *Arabidopsis* Sar1 homologs in ER protein export, the conserved tyrosine 84 on AtSar1c was mutated to cysteine or alanine as indicated (*SI Appendix*, Fig. S4*B*). When coexpressed with these AtSar1cDN mutant constructs, vacuolar cargo was delivered normally to the vacuole in *Arabidopsis* protoplasts (*SI Appendix*, Fig. S4 *D* and *E*). To confirm that the above observations derived from protoplasts were also true for intact plants, transgenic *Arabidopsis* plants expressing AtSar1aDN C84Y-GFP, AtSar1cDN Y84C-GFP, and AtSar1cDN Y84A-GFP driven by a DEX-inducible promoter were generated for subsequent analysis. Upon DEX treatment, ER export of Aleurain-mRFP was inhibited in the dex::AtSar1aDN C84Y-GFP transgenic plants (Fig. 2*Ad*), whereas Aleurain-mRFP still reached the vacuole normally in the dex::AtSar1cDN Y84C-GFP and AtSar1cDN Y84A-GFP mutants (Fig. 2 *Ae* and *Af*). Cargo secretion assays using Myc-tag AtSar1a/cDN and their mutant constructs further showed that Aleurain-GFP was degraded mainly to the GFP core in the vacuole when coexpressed with AtSar1aDN-myc and AtSar1aDN C84A-myc, whereas expression of AtSar1aDN C84Y-myc caused most full-length Aleurain-GFP to be retained in the protoplasts (Fig. 2 *B* and *C*). Additionally, AtSar1cDN-myc caused most full-length Aleurain-GFP to be retained in the ER, whereas Aleurain-GFP was largely degraded to the GFP core as against AtSar1cDN Y84C-myc and AtSar1cDN Y84A-myc (Fig. 2 *B* and *C*). We next examined the distinct effects of the AtSar1a/c mutants on ER membrane cargo export. Consistent with the vacuolar cargo, the ER export of the plasma membrane cargo

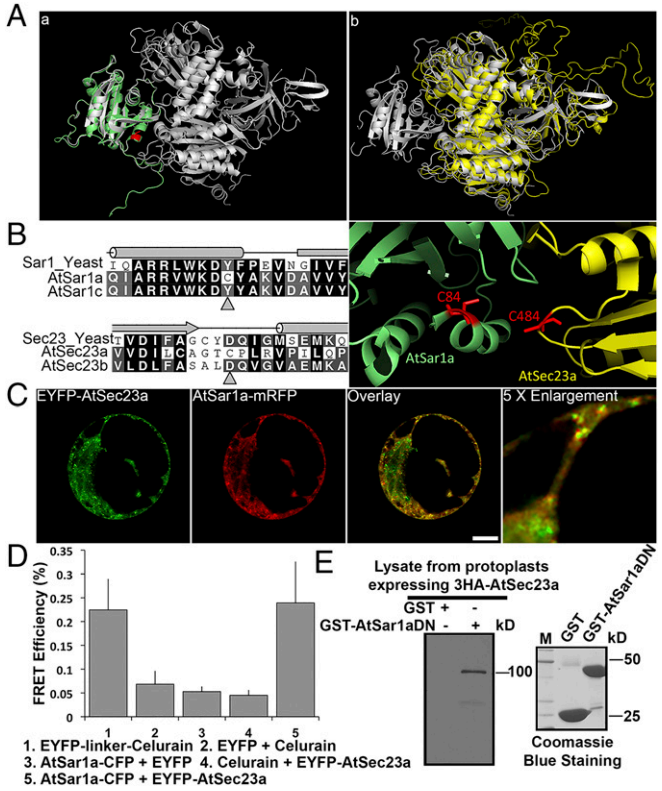

Fig. 3. AtSar1a specifically interacts with the unique plant COPII inner coat protein AtSec23a. (*A*) By homology modeling, the structures of *Arabidopsis* (*a*) AtSar1a (green) and AtSec23a (yellow) were predicted using the yeast Sar1-Sec23 crystal structure (white, Protein Data Bank code 2QTV) as template. The predicted structures were then aligned to the yeast Sar1-Sec23 structure. (*B*) Sequence alignment of AtSar1a, AtSar1c with yeast homolog Sar1 and AtSec23a, and AtSec23b with yeast homolog Sec23. The selected part of alignment is shown. Triangles indicate changes of the corresponding residues in AtSar1a and AtSec23a. Enlarged image showing specific interaction pair of AtSar1a (green) and AtSec23a (yellow). Cys84 in AtSar1a and Cys484 in AtSec23a are labeled in red. (*C*) Colocalization of AtSar1a and AtSec23a in *Arabidopsis* protoplasts. (Scale bar, 10 μm.) (*D*) FRET analysis showed direct interactions between AtSar1a and AtSec23a in *Arabidopsis*. (*E*) Pull-down assay showing the interaction between AtSar1a and AtSec23a. GST and GST-AtSar1aDN beads were incubated with lysates from protoplasts expressing 3HA-AtSec23a. Bound proteins were visualized by immunoblot with HA antibody.

BRi1-mRFP was inhibited when coexpressed with AtSar1cDN and AtSar1aDN C84Y in *Arabidopsis* protoplasts (*SI Appendix*, Fig. S6 *A*, *C*, and *F*). Nevertheless, AtSar1aDN, AtSar1cDN Y84C, and AtSar1cDN Y84A showed reduced ability in inhibiting membrane protein ER export as BRi1-mRFP exhibited a plasma membrane pattern (*SI Appendix*, Fig. S6 *B*, *D*, *E*, and *F*). In addition, BRi1-mRFP still trafficked to the plasma membrane when coexpressed with other point mutation constructs of AtSar1aDN (*SI Appendix*, Fig. S7). Similar results were obtained in using cysteine protease and AtSCAMP as additional vacuolar and membrane cargoes, respectively, in identical experiments (*SI Appendix*, Fig. S8). Taken together, we have identified a single amino acid that is responsible for causing the functional heterogeneity of small GTPase Sar1 homologs in plants.

AtSar1a Interacts with the Unique Plant COPII-Inner Coat Protein AtSec23a. Previously, a hydrophobic triad was identified in the mammalian ADP ribosylation factor (Arf) family proteins and was proposed to be a major structural determinant for effector specificity (27). The Arf relative protein Sar1 also contains this hydrophobic triad, which is strictly conserved in mammals and yeast. Interestingly, both cysteine 84 in AtSar1a and tyrosine 84 in AtSar1c are residues within the hydrophobic triad (*SI Appendix*, Fig. S9*A*), indicating the possibility of recognition of AtSar1a or AtSar1c by specific AtSec23 homologs. Protein structure homology modeling was used to pin point the possible role of Cys84 on AtSar1a as the structures of yeast Sar1 and the Sar1-Sec23/Sec24 prebudding complex have been reported (7). Indeed, we found that the Cys84 in AtSar1a and Tyr84 in AtSar1c were adjacent to switch II and contact primarily by the trunk domain of the yeast Sar1-GAP Sec23 (Fig. 3*Aa* and *SI Appendix*, Fig. S9*C*). Furthermore, we found that the Cys84 in AtSar1a and Tyr84 in AtSar1c were close to Asp351 in yeast Sec23 (Fig. 3Aa and *SI Appendix*, Fig. S9*C*), which has been shown to contribute to the interaction with Sar1 (*SI Appendix*, Fig. S10*Aa*) (7). Sequence alignment of *Arabidopsis* Sec23 homologs with yeast Sec23 indicated that most AtSec23 homologs, such as AtSec23b, contained the conserved aspartate at that position (*SI Appendix*, Fig. S9*B*). Strikingly, the uncharacterized *Arabidopsis* Sec23 homolog AtSec23a has an amino acid substitution from aspartate to cysteine at that position (*SI Appendix*, Fig. S9*B*). Through the structure modeling, we found that this amino acid, cysteine 484 on AtSec23a, was indeed the closest amino acid facing cysteine 84 in AtSar1a (Fig. 3 *Ab* and *B*). We hypothesized that AtSar1a and AtSec23a might form a specific Sar1-Sec23 pair in plants. When transiently coexpressed in *Arabidopsis* protoplasts, EYFP-AtSec23a showed clear punctae that substantially colocalized with AtSar1a-mRFP (Fig. 3*C*). Acceptor photobleaching-fluorescence resonance energy transfer (FRET-AB) analysis further confirmed an in vivo interaction between AtSar1aDN and AtSec23a because they exhibited high

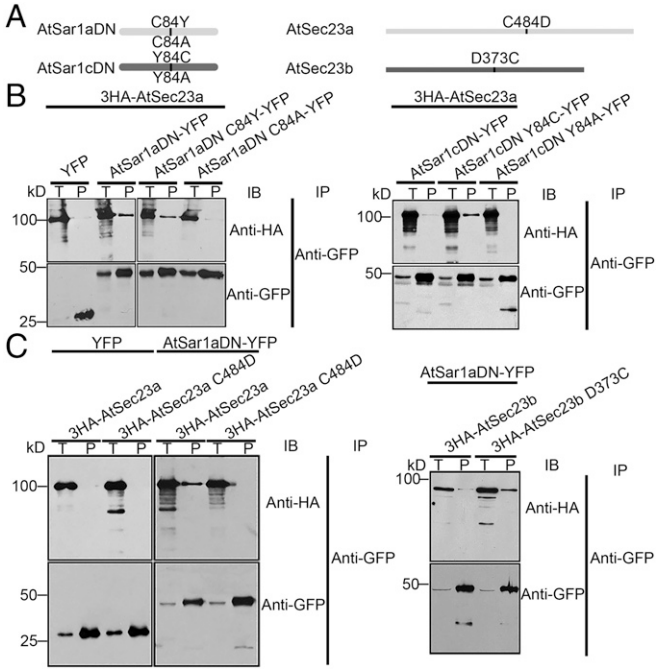

Fig. 4. Cys84 in AtSar1a and Cys484 in AtSec23a are crucial for the specific interaction. (*A*) Diagram showing the mutant constructs used for the immunoprecipitation (IP) assay. (*B*) IP assay showing that cysteine 84 in AtSar1a is crucial for the interaction with AtSec23a. *Arabidopsis* protoplasts coexpressing 3HA-AtSec23a with YFP only or indicated YFP fusions of AtSar1 variants were subjected to protein extraction and IP with GFP-trap followed by immunoblotting with indicated antibodies. (*C*) IP assay showing that cysteine 484 in AtSec23a is essential for the specific interaction with AtSar1a. *Arabidopsis* protoplasts coexpressing AtSar1aDN-YFP or YFP with indicated HA-tagged AtSec23 variants were subjected to protein extraction and IP with GFP-trap followed by immunoblotting with indicated antibodies.

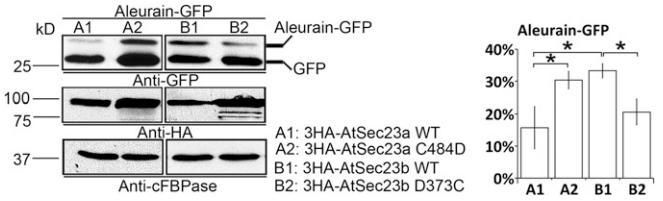

Fig. 5. Cys484 in AtSec23a is essential for its distinct function with AtSar1a on ER cargo export. *Arabidopsis* protoplasts coexpressing Aleurain-GFP with the indicated HA-tagged AtSec23 variants were subjected to protein extraction followed by immunoblotting with the indicated antibodies. The relative grayscale intensity (scale 0–100%) of the Aleurain-GFP and GFP core was quantified using ImageJ software in which the combinatorial intensity of both proteins was expressed as 100%. Data represent mean ± SD; $*P < 0.05$ (ANOVA with Scheffé test).

FRET efficiency as the positive control (Fig. 3*D*). On the other hand, we found that the purified GST-AtSar1aDN but not GST can pull down the 3HA-AtSec23a from the electroporated protoplasts in vitro (Fig. 3*E*). Thus, we demonstrated that AtSar1a specifically recognizes AtSec23a, a unique plant Sec23 homolog.

Cys84 on AtSar1a and Cys484 on AtSec23a Are Essential for the Specific Pairing. In yeast, Tyr65 of Sar1 (corresponds to Cys84 in AtSar1a and Tyr84 in AtSar1c) forms a hydrogen bond to Asp351 of Sec23 (Cys484 in AtSec23a and Asp373 in AtSec23b) (*SI Appendix*, Fig. S10*Aa*). Interestingly, structural modeling suggests that this hydrogen bond is conserved in the AtSar1c/AtSec23b pair (*SI Appendix*, Fig. S10*Ab*) but not in the AtSar1a/AtSec23a pair (*SI Appendix*, Fig. S10*Ac*). It has been well established that burial of polar groups (i.e., hydroxyl group of tyrosine and carboxylate group of aspartate in the Sar1/Sec23 interface) is favorable only when it is compensated by a hydrogen bond (28). So we hypothesized that AtSar1c and AtSec23b (accession no. At1g05520) should form specific pairwise interactions, such as that in the yeast Sar1/Sec23 pair. By the same argument, AtSar1a and AtSec23a should interact with one another (Fig. 3) because the polar residues (tyrosine and aspartate) are replaced by cysteine, a nonpolar residue, that can be favorably buried in the Sar1/Sec23 interface. Consistent with this hypothesis, we showed that AtSar1cDN was immunoprecipitated with AtSec23b (*SI Appendix*, Fig. S10*C*) and AtSar1aDN with AtSec23a (Fig. 4*B*). Furthermore, coimmunoprecipitation of AtSar1cDN/AtSec23a (Fig. 4*B*) and AtSar1aDN/AtSec23b (Fig. 4*C*) was strongly impaired, suggesting that AtSar1a specifically interacts with AtSec23a and AtSar1c with AtSec23b.

To further prove that Cys84/Cys484 of AtSar1a/AtSec23a are necessary and sufficient for the specific pairwise interaction, we performed coimmunoprecipitation with the indicated mutant constructs using *Arabidopsis* protoplasts (Fig. 4*A*). Coimmunoprecipitation was observed (*SI Appendix*, Fig. S10*C*) for all variants of AtSar1/AtSec23 retaining the Tyr-Asp pair of residues (*SI Appendix*, Fig. S10*B*, panel 1). When either of the tyrosine and aspartate residues were replaced by cysteine (*SI Appendix*, Fig. S10*B*, panels 3 and 4), coimmunoprecipitation between variants of AtSar1/AtSec23 was strongly impaired (Fig. 4 *B* and *C*; *SI Appendix*, Fig. S10 *D* and *E*). These results suggest that burial of Tyr84 and Asp373/484 in the Sar1/Sec23 interface is not favorable unless it is compensated by a hydrogen bond between these two polar residues (*SI Appendix*, Fig. S10*B*). On the other hand, coimmunoprecipitation was retained (Fig. 4 *B* and *C*; *SI Appendix*, Fig. S10*D*) when both residues were replaced by cysteine (*SI Appendix*, Fig. S10*B*, panel 2), suggesting that burial of two nonpolar cysteine residues is favorable in the Sar1/Sec23 interface. Based on the structure modeling, the two cysteine residues are unlikely to form a disulfide bond because they are too far away from each other (*SI Appendix*, Fig. S10*Ac*). When Tyr84 on AtSar1c or Cys84 on AtSar1a was replaced by alanine, there was no interaction between AtSar1 and AtSec23a (Fig. 4*B*). Based on the structure modeling, the –SH group of Cys84 is in close contact with Leu71 of AtSar1. It is likely that the truncation of Cys84 to alanine may disrupt the local structure of the AtSar1 and sever its interaction with AtSec23a (*SI Appendix*, Fig. S10*B*, panel 5). Our results are consistent with the conclusions that (*i*) Cys84 in AtSar1a and Cys484 in AtSec23a are crucial for the plant-specific Sar1-Sec23 pair formation; (*ii*) the specific interaction is caused by burial of two nonpolar cysteine residues in the Sar1/Sec23 interface; and (*iii*) nonspecific interactions, such as AtSar1a/AtSec23b or AtSar1c/AtSec23a, are prevented by unfavorable burial of Tyr84 of AtSar1c or Asp373 of AtSec23b in the interface.

Cys484 Is Essential for the Distinct Function of AtSec23a in ER Export. A previous study indicated that COPII tethering and fusion was completely blocked in the presence of excess Sec23p in vitro (29). To evaluate the effects of the corresponding amino acid in AtSec23a on cargo ER export, we coexpressed the soluble cargo Aleurain-GFP with indicated mutants of AtSec23a and AtSec23b in *Arabidopsis* protoplasts. Immunoblot analysis showed that AtSec23a exhibited mild effects on ER vacuolar cargo export because the full-length Aleurain-GFP was degraded mainly to the GFP core (Fig. 5). Interestingly, AtSec23a C484D can trap the Aleurain-GFP in ER as AtSec23b, whereas most of the Aleurain-GFP was degraded to the GFP core as against AtSec23a and AtSec23b D373C (Fig. 5). These results demonstrated that Cys484 in AtSec23a determined a similar function on cargo ER export as AtSar1a.

ER Export of bZIP28 Is Affected by AtSar1aDN Under ER Stress. Interestingly, the unique AtSar1a/AtSec23a pair, but not the other Sar1 and Sec23 homologs, were recently shown to be bZIP28-dependent ER stress-responsive genes in a microarray analysis (30). bZIP28, an ER resident stress sensor/transducer related to the mammalian ATF6, is exported from the ER to the

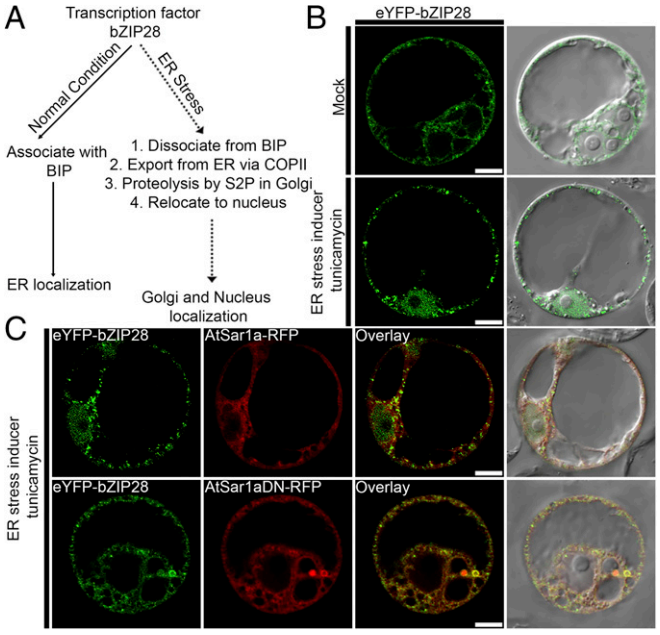

Fig. 6. bZIP28 is a cargo of AtSar1a under ER stress. (*A*) Model of bZIP28 trafficking in response to ER stress. (*B*) eYFP-bZIP28 localized to the ER under normal conditions (*Top*) and transported to Golgi and the nucleus under ER stress (*Bottom*). (Scale bars, 10 μm.) (*C*) AtSar1aDN inhibited ER export of bZIP28 under ER stress. eYFP-bZIP28 and AtSar1a (*Top*) or AtSar1aDN (*Bottom*) were cotransfected in *Arabidopsis* protoplasts for 6–8 h, followed by treatment with 5 μg/mL tunicamycin for 2 h before confocal imaging. (Scale bars, 10 μm.)

Golgi via COPII vesicles under ER stress (Fig. 6*A*) (31). To test if bZIP28 is a cargo of AtSar1a-mediated ER export under ER stress, we coexpressed eYFP-bZIP28 with AtSar1a-RFP or AtSar1aDN-RFP in *Arabidopsis* protoplasts upon ER stress induced by tunicamycin treatment. When expressed in *Arabidopsis* protoplasts, bZIP28 remained mainly in the ER under normal conditions but exited the ER to show Golgi and nucleus labeling upon ER stress induction by tunicamycin (Fig. 6*B*). However, the tunicamycin-induced ER export (and its subsequent Golgi and nucleus localization) of bZIP28 was inhibited in cells coexpressing AtSar1aDN but not AtSar1a (Fig. 6*C*), indicating that bZIP28 may be a cargo of AtSar1a-mediated ER export under ER stress in plant cells. Future studies will focus on exploring its physiological and functional significance in plants.

In summary, we have demonstrated that the *Arabidopsis* Sar1 homolog AtSar1a localizes to distinct ERESs that are closely associated with Golgi stacks, indicating a specific function in protein ER export. Indeed, AtSar1a exhibited distinct effects on vacuolar and membrane cargo secretion in *Arabidopsis* plants. Such distinct effects on ER cargo export are determined by a single amino acid substitution from the conserved tyrosine to cysteine in the hydrophobic triad. Although the hydrophobic triad has been proposed to be a structural determinant for effector specificity, the amino acids that consist of the hydrophobic triad are invariant in most mammalian Arf family proteins including the Arf relative protein Sar1 (27). The fact that AtSar1a contains an amino acid substitution in the hydrophobic triad points to the existence of a corresponding unique Sar1-effector Sec23 in the *Arabidopsis* genome. Strikingly, among the seven Sec23 homologs in *Arabidopsis*, we identified an uncharacterized Sec23, namely AtSec23a, containing a corresponding amino acid substitution from the conserved aspartate to cysteine in the trunk domain closest to Cys84 on AtSar1a. An interaction between AtSar1a and AtSec23a places them as a unique pair of Sar1 and Sar1-GAP in the plant COPII machinery. Both amino acid substitutions on AtSar1a and AtSec23a are essential for the specific pair, as evidenced by the mutagenesis and interaction study. Consistent with this, we have shown that AtSec23a exhibits a distinct function with AtSar1a on ER vacuolar cargo export and that this is determined by the specific amino acid substitution on AtSec23a. Despite increasing progress being made in our understanding of the importance of COPII subunit diversity in eukaryotes, the mechanisms underlying the functional heterogeneity have remained unknown. Our studies have thus unveiled a previously unidentified molecular basis for COPII functional diversity. Because only AtSar1a and AtSec23a have a unique amino acid substitution among eukaryotes, we postulate that this pair may perform a specific distinct function in plants. Interestingly, the unique pair AtSar1a-AtSec23a are ER stress-responsive genes. Our data indicate that the unique pair may be essential for the ER export of the ER resident stress sensor/transducer bZIP28 under stress conditions. Future studies will focus on testing whether AtSec23a can cooperate with AtSar1a and control the formation of COPII vesicles for distinct cargos under stress conditions in plants. Moreover, multiple biochemical assays and cellular/protemoic approaches will be established to identify additional unique cargos for functional studies in plants.

Materials and Methods

Additional materials and methods including plant materials, antibodies, plasmid construction, immunofluorescent labeling, drug treatment, particle bombardment of *Arabidopsis* seedlings, *Arabidopsis* protoplast transient expression, structure modeling, pull-down assay, immunoprecipitation, acceptor photobleaching FRET analysis, confocal microscopy, and SIM are described in *SI Appendix, SI Materials and Methods*.

ACKNOWLEDGMENTS. We thank Mr. Lai Chun Hei (Department of Physics, The Chinese University of Hong Kong) for technical support in using the structured illumination microscopy. This work was supported by grants from the Research Grants Council of Hong Kong (CUHK466011, 465112, 466613, 14109315, CUHK2/CRF/11G, C4011-14R, HKUST10/CRF/12R, HKUST12/CRF/13G, and AoE/M-05/12), National Natural Science Foundation of China (NSFC)/Research Grants Council (N_CUHK406/12), NSFC (31270226 and 31470294), Chinese Academy of Sciences-Croucher Joint Lab Scheme, and the Shenzhen Peacock Project (KQTD201101).

1. Novick P, Field C, Schekman R (1980) Identification of 23 complementation groups required for post-translational events in the yeast secretory pathway. *Cell* 21(1):205–215.
2. Barlowe C, et al. (1994) COPII: A membrane coat formed by Sec proteins that drive vesicle budding from the endoplasmic reticulum. *Cell* 77(6):895–907.
3. Nakańo A, Muramatsu M (1989) A novel GTP-binding protein, Sar1p, is involved in transport from the endoplasmic reticulum to the Golgi apparatus. *J Cell Biol* 109(6 Pt 1):2677–2691.
4. Nakano A, Brada D, Schekman R (1988) A membrane glycoprotein, Sec12p, required for protein transport from the endoplasmic reticulum to the Golgi apparatus in yeast. *J Cell Biol* 107(3):851–863.
5. Yoshihisa T, Barlowe C, Schekman R (1993) Requirement for a GTPase-activating protein in vesicle budding from the endoplasmic reticulum. *Science* 259(5100):1466–1468.
6. Miller E, Antonny B, Hamamoto S, Schekman R (2002) Cargo selection into COPII vesicles is driven by the Sec24p subunit. *EMBO J* 21(22):6105–6113.
7. Bi X, Corpina RA, Goldberg J (2002) Structure of the Sec23/24-Sar1 pre-budding complex of the COPII vesicle coat. *Nature* 419(6904):271–277.
8. Zanetti G, Pahuja KB, Studer S, Shim S, Schekman R (2012) COPII and the regulation of protein sorting in mammals. *Nat Cell Biol* 14(1):20–28.
9. Jones B, et al. (2003) Mutations in a Sar1 GTPase of COPII vesicles are associated with lipid absorption disorders. *Nat Genet* 34(1):29–31.
10. Robinson DG, Herranz M-C, Bubeck J, Pepperkok R, Ritzenthaler C (2007) Membrane dynamics in the early secretory pathway. *Crit Rev Plant Sci* 26(4):199–225.
11. Faso C, et al. (2009) A missense mutation in the Arabidopsis COPII coat protein Sec24A induces the formation of clusters of the endoplasmic reticulum and Golgi apparatus. *Plant Cell* 21(11):3655–3671.
12. Nakano RT, et al. (2009) GNOM-LIKE1/ERMO1 and SEC24a/ERMO2 are required for maintenance of endoplasmic reticulum morphology in Arabidopsis thaliana. *Plant Cell* 21(11):3672–3685.
13. Hanton SL, et al. (2008) Plant Sar1 isoforms with near-identical protein sequences exhibit different localisations and effects on secretion. *Plant Mol Biol* 67(3):283–294.
14. Brandizzi F, Barlowe C (2013) Organization of the ER-Golgi interface for membrane traffic control. *Nat Rev Mol Cell Biol* 14(6):382–392.
15. Ito Y, et al. (2012) cis-Golgi proteins accumulate near the ER exit sites and act as the scaffold for Golgi regeneration after brefeldin A treatment in tobacco BY-2 cells. *Mol Biol Cell* 23(16):3203–3214.
16. Robinson DG, Brandizzi F, Hawes C, Nakano A (2015) Vesicles versus tubes: Is endoplasmic reticulum-Golgi transport in plants fundamentally different from other eukaryotes? *Plant Physiol* 168(2):393–406.
17. Ito Y, Uemura T, Nakano A (2014) Formation and maintenance of the Golgi apparatus in plant cells. *Int Rev Cell Mol Biol* 310:221–287.
18. Yang YD, et al. (2005) Dynamics of COPII vesicles and the Golgi apparatus in cultured Nicotiana tabacum BY-2 cells provides evidence for transient association of Golgi stacks with endoplasmic reticulum exit sites. *Plant Cell* 17(5):1513–1531.
19. Zhang C, Kotchoni SO, Samuels AL, Szymanski DB (2010) SPIKE1 signals originate from and assemble specialized domains of the endoplasmic reticulum. *Curr Biol* 20(23):2144–2149.
20. daSilva LL, et al. (2004) Endoplasmic reticulum export sites and Golgi bodies behave as single mobile secretory units in plant cells. *Plant Cell* 16(7):1753–1771.
21. Bar-Peled M, Raikhel NV (1997) Characterization of AtSEC12 and AtSAR1. Proteins likely involved in endoplasmic reticulum and Golgi transport. *Plant Physiol* 114(1):315–324.
22. Aridor M, Balch WE (2000) Kinase signaling initiates coat complex II (COPII) recruitment and export from the mammalian endoplasmic reticulum. *J Biol Chem* 275(46): 35673–35676.
23. Takagi J, et al. (2013) MAIGO5 functions in protein export from Golgi-associated endoplasmic reticulum exit sites in Arabidopsis. *Plant Cell* 25(11):4658–4675.
24. Castillon GA, Watanabe R, Taylor M, Schwabe TM, Riezman H (2009) Concentration of GPI-anchored proteins upon ER exit in yeast. *Traffic* 10(2):186–200.
25. Takeuchi M, et al. (2000) A dominant negative mutant of sar1 GTPase inhibits protein transport from the endoplasmic reticulum to the Golgi apparatus in tobacco and Arabidopsis cultured cells. *Plant J* 23(4):517–525.
26. Honda A, Al-Awar OS, Hay JC, Donaldson JG (2005) Targeting of Arf-1 to the early golgi by membrin, an ER-Golgi SNARE. *J Cell Biol* 168(7):1039–1051.
27. Chavrier P, Ménétrey J (2010) Toward a structural understanding of arf family:effector specificity. *Structure* 18(12):1552–1558.
28. Loladze VV, Ermolenko DN, Makhatadze GI (2002) Thermodynamic consequences of burial of polar and non-polar amino acid residues in the protein interior. *J Mol Biol* 320(2):343–357.
29. Cai H, et al. (2007) TRAPPI tethers COPII vesicles by binding the coat subunit Sec23. *Nature* 445(7130):941–944.
30. Song ZT, et al. (2015) Transcription factor interaction with COMPASS-like complex regulates histone H3K4 trimethylation for specific gene expression in plants. *Proc Natl Acad Sci USA* 112(9):2900–2905.
31. Srivastava R, Chen Y, Deng Y, Brandizzi F, Howell SH (2012) Elements proximal to and within the transmembrane domain mediate the organelle-to-organelle movement of bZIP28 under ER stress conditions. *Plant J* 70(6):1033–1042.